In vivo optochemical control of cell contractility at single cell resolution by Ca^{2+} induced myosin activation

Deging Kong [(1)], Fred Wolf [(2)], Jörg Großhans [(1)]*

(1) Institute for Developmental Biochemistry, University of Göttingen, Justus-von-Liebig Weg 11, 37077 Göttingen, Germany.
(2) Max Planck Institute for Dynamics and Self-Organization (MPI-DS), Bernstein Center for Computational Neuroscience Göttingen, Faculty of Physics, University of Göttingen, Am Faßberg 17, 37077 Göttingen, Germany.
Correspondence and requests for materials should be addressed to J. G. (jgrossh@gwdg.de)

Abstracts

The spatial and temporal dynamics of cell contractility plays a key role in tissue morphogenesis, wound healing and cancer invasion. Here we report a simple, single cell resolution, optochemical method to induce reversible minute-scale cell contractions *in vivo* during morphogenesis. We employed the photolabile Ca^{2+} chelator *o*-nitrophenyl EGTA to induce bursts of intracellular free Ca^{2+} by laser photolysis. Ca^{2+} bursts appear within seconds and are restricted to individual target cells. Cell contraction reliably followed within a minute, to about half of the cross-sectional area. Increased Ca^{2+} levels and contraction were reversible and the target cells further participated in tissue morphogenesis. Cell contractions are paralleled with non-muscle myosin-II accumulation in the apico-medial cortex, indicating that Ca^{2+} bursts trigger non-muscle myosin II activation. Our approach can be easily adapted to many experimental systems and species, as no specific genetic elements are required and a widely used reagent is employed.

Introduction

Contractility underlies manifold processes in cell and tissue morphogenesis, including cell migration, cell shape changes, or junction collapse [1-4]. In epithelial tissues, cell contractions impact on neighboring cells by mechanically pulling on

neighbors via adherens junctions. The mechanical link may elicit a specific response in neighbors and may thus positively or negatively affect contractility in neighbors in a non-autonomous manner [5]. Within a tissue, such cell-cell interactions can contribute to emergent tissue behavior, such as folds and furrows. The function of mutual cell-cell interactions is difficult to study by classical genetic approaches. What are needed are acute interventions with high temporal and spatial resolution, ideally in the scale of seconds and of individual cells.

For controlling cell contractility optogenetic approaches have recently been developed. Cell contractility can be inhibited by optically induced membrane recruitment of $PI(4,5)P_2$ leading to interference with phosphoinositol metabolism and subsequent suppression of cortical actin polymerization [6]. Optical activation of contractility has been achieved by light-induced activation of the Rho-Rok pathway, which controls Myosin II based contractility [7,8]. Despite their effectiveness, optogenetic methods require expression of modified proteins such as light-sensitive and dimerization domains, which need to be introduced into the genetic background of the experimental organisms. Furthermore, the used chromophores absorb light in the visible spectrum, which restricts the choice of labels and reporters for cell imaging.

Optochemical methods represent an alternative to genetically encoded sensor and effector proteins [9]. Intracellular calcium ions (Ca^{2+}) are known to be an important regulator of contractility in many cell types. Ca^{2+} not only plays a central role in muscle contraction, but also in cultured epithelial cells [10], in amnioserosa cells during dorsal closure [11], during neural tube closure [12,13] and in the folding morphogenesis of the neural plate [14]. In *Drosophila* oogenesis, tissue wide increase of intracellular Ca^{2+} activates Myosin II and impairs egg chamber elongation [15]. Furthermore a transient increase in Ca^{2+} concentration induces apical constriction in cells of the neural tube in *Xenopus* [16]. While the molecular mechanism of Ca^{2+} contraction coupling in non-muscle cells remains to be precisely understood, Ca^{2+} contraction coupling offers a simple and temporally precise way to interface and control contractile activity. In neuroscience, optochemical methods for the release of intracellular Ca^{2+} are well established and widely employed e.g. in biophysical studies of synaptic transmission

[17]. Here we report a Ca^{2+} uncaging method to control epithelial cell contractility on the scale of seconds and at single cell resolution during tissue morphogenesis in *Drosophila* embryos and has minimal spectral overlap with fluorescent protein reporters. Our results provide evidence for a specific effect of increased intracellular Ca^{2+} on activating non-muscle myosin II and its recruitment to the actomyosin cortex.

Results

Uncaging induces a rapid Ca^{2+} burst in epithelial cells in *Drosophila* embryos.

Photolysis of the Ca^{2+} chelator *o*-nitrophenyl EGTA (NP-EGTA) [18] (Fig. 1A) is widely used in neurobiology for the modulation of intracellular Ca^{2+} concentration [19,20]. Here, we employed the membrane-permeant acetoxymethyl (AM) ester derivative, which complexes Ca^{2+} once the AM moiety is removed by intracellular esterases. Following microinjection into staged embryos, uncaging was induced in the focal volume of a pulsed 355 nm laser beam (Fig. 1B). In our setup, the light paths of the UV laser and the recording laser in the visible spectrum were controlled independently, which allowed concomitant uncaging and imaging. We conducted our experiments in the lateral epidermis of *Drosophila* embryos during the gastrulation stage. The epidermis during this stage constitutes a columnar epithelium with a cell diameter in the range of about 8 µm and cell height of about 25 µm.

To visualize and assess changes of intracellular Ca^{2+} dynamics following uncaging, we employed a genetically encoded Ca^{2+} sensor protein, GCaMP6. Embryos expressing a membrane bound, myristoylated variant of GCaMP6 [21] were injected with NP-EGTA-AM and subjected to uncaging. We observed a transient increase of GCaMP6 fluorescence within a second specifically in the cell targeted with UV light pulses (Fig. 1C, Supp. movie 1). Quantification showed a fourfold increase of GCaMP fluorescence (F/F0) after two seconds. Afterwards, the GCaMP fluorescence gradually decreased to initial levels within a few minutes (Fig. 1E). We did not detect an increase of GCaMP fluorescence after UV exposure in control embryos injected with buffer only (Fig. 1D, E).

The increase in Ca^{2+} sensor signal was restricted to the single target cell (Fig. 1C, Supp. movie 1). The Ca^{2+} sensor signal in the next neighbors and next-next neighbors showed fluctuations, which did not change over time and were comparable to control embryos (Fig. 1F). In summary, these experiments show that epithelial tissue in *Drosophila* embryos is susceptible to Ca^{2+} uncaging. Uncaging leads to a reversible, second-scale increase of intracellular Ca^{2+} levels restricted to the target cell. The magnitude of the Ca^{2+} increase is comparable to what was previously reported for neuronal cells [20].

Ca^{2+} bursts induce transient cell contraction.

We next investigated the consequence of Ca^{2+} bursts on cell shape. We conducted uncaging in embryos expressing E-Cad-GFP, which labels adherens junctions and thus cell junctions at a subapical position. Strikingly, we detected a contraction of the target cell to about half of the cross-sectional area (Fig. 2A, Supp. movie 2). Target cells in control embryos injected with buffer remained largely unaffected (Fig. 2B). This was confirmed by quantification of the cross sectional areas. Similar to unexposed cells, target cells in buffer-injected embryos undergo regular cell shape changes with an amplitude of about 10–20% (Fig. 2C and S1B)[22,23]. All target cells with Ca^{2+} bursts contracted by about 50% within 1–2 minutes (Fig. 2C and S1A). After 3 minutes, some of the target cells started to re-expand, albeit they did to reach their original cross-sectional area in 5 minutes (Fig. S1A).

Exposure to UV laser and Ca^{2+} uncaging did not affect further development of the target cells and surrounding tissue. We tracked target cells over an extended period of 15 min by time lapse imaging (Fig. 2D, E). Following initial contraction during the first two minutes after UV laser exposure, the target cell relaxed to almost initial size and showed typical oscillations with periods of a few minutes and amplitudes of 10–20% (Fig. 2D, E) [22,23]. We did not observe that target cells were extruded or got lost from epithelia tissue. This behavior indicates that the Ca^{2+} induced contraction was transient and target cells remained integrated in the epithelial tissue (Fig. 2D).

Modulation of UV laser exposure

We modulated the effect on contractility by varying the focal volume of the UV laser (spot radius). Variation of laser power or illumination time in contrast proved difficult, as either the response was lost or became too strong. With an increase in focal volume, we observed a faster response in contraction. A spot radius of 4 or 1 initiated contraction within about 1 or 2.5 min, respectively. With both settings, a final contraction to about half the cell area was reached after 2.5 min or 4–5 min, respectively (Fig. 3A). For these studies two target cells were exposed to UV laser sequentially within 10 seconds and varying focal volumes (Fig. 3B, 3C, Supp. movie 3). The larger focal volume by a larger spot radius led a faster response but not a higher degree of contraction by the cell. Our experiments thus indicate that the dynamics of contraction can be modulated by varying the uncaging settings.

Role of Myosin II in Ca^{2+} induced cell contraction.

Multiple mechanisms are conceivable for Ca^{2+} induced cell contraction. Given the time scale in the minute range, it is unlikely that slow transcriptional or translational processes are involved. It is also unlikely that Ca^{2+} directly activates contraction similar to its role in muscle cells due to the time lag between Ca^{2+} increase and contraction of the cell. In principle, a change in cell volume may involve Ca^{2+} induced efflux of water, for example. Alternatively, Ca^{2+} may activate myosin II, comparable to what has been reported for the *Drosophila* egg chamber[15]. Such a specific Myosin II activation may be mediated via Rho-Rok signaling or via Ca^{2+} dependent protein kinases or phosphatases, such as myosin light chain kinase (MLK) [24].

As a first step to identifying the mechanism of Ca^{2+} induced cell contraction, we imaged myosin II dynamics following uncaging in embryos expressing E-Cad-GFP to label cell-cell contacts and sqh-mCherry (myosin regulatory light chain) (Fig. 4). sqh-mCherry fluorescence is a direct indicator of active myosin II mini filaments, which are visible as clusters. Myosin II is found at the adherens junctions (junctional pool) and at the apical cortex (medial pool), where it is responsible for apical constriction [25]. We focused on the medial pool of myosin II. To compensate bleaching of the sqh-mCherry signal in target cells, we normalized fluorescence to the time after UV exposure in

embryos with and without uncaging. We observed an increase of sqh-mCherry fluorescence after about 0.5 to 1 min in target cells in embryos with the cage and a continuous decrease of fluorescence in control embryos (Fig. 4C). These observations provide strong evidence that Ca^{2+} uncaging triggers myosin II activation on the same time scale as cell contraction.

Discussion

We developed and validated Ca^{2+} uncaging as an optochemical method to induce cell contraction in epithelial tissues with precise temporal and spatial control. This approach enabled us to induce Ca^{2+} bursts in selected single cells within seconds and leading to contraction to about half of the cross sectional area within 1 minute. The induced contraction was reversible and did not perturb tissue integrity. To our best knowledge, this is the first report for optically controlled cell contraction on the minute scale and at single cell resolution *in vivo* during epithelial tissue morphogenesis.

The optochemical system that we use is based on photolabile Ca^{2+} chelators and a pulsed UV laser. The cage compound “NP-EGTA, AM” is membrane-permeant and thus allows convenient application to whole tissues. The 355nm UV laser we used is compatible with modern objectives and can be conveniently mounted on conventional live imaging microscopes. The dose of UV light depends on factors like light scattering by the tissue and thickness of the sample and needs to be carefully adjusted for the experimental system. Using a fluorescent Ca^{2+} sensor protein provides a direct optical readout of Ca^{2+} release and greatly aids UV intensity adjustment.

Importantly, Ca^{2+} uncaging does not require any genetically encoded protein, thus accelerating the active screening for mechanobiological cellular pathways and components, e. g. by comparing wide arrays of mutants to wild type behavior. In addition, Ca^{2+} uncaging is likely to open applications in the manifold experimental systems with low genetic tractability. Importantly, UV Ca^{2+} uncaging leaves the entire visible spectrum available for optical interfacing with florescent protein indicators and opsin-based effectors. This in particular increases the options for simultaneously

recording of cell and tissue behavior with the large palette of available fluorescent protein tags from CFP to RFP.

Ca^{2+} uncaging appears particularly suitable for studies of tissue morphogenesis. Specifically, intercellular coupling between neighboring cells poses a challenge for the experimental design in tissue morphogenesis. Here cause and consequence cannot be easily distinguished without targeted activation of cellular contractility and precise external control of cellular behaviors by acute interference is mandatory for dissecting functional dependencies. Although the mechanistic details for Ca^{2+} induced contraction need to be further resolved, UV induced Ca^{2+} uncaging allows interference with the mechanics of tissues with appropriate temporal and high spatial resolution. The method can be applied to a wide range of processes and organisms and should greatly improve our ability to study the causal role of cell contractility and of tissue mechanics *in vivo*.

Materials and Methods

Fly Strains

Fly stocks were obtained from the Bloomington Drosophila Stock Center, if not otherwise noted and genetic markers and annotations are described in Flybase [26]. Following transgenes were used UASp-GCaMP6-myr [21], E-Cadherin-GFP [27], ubiquitin-E-Cadherin-GFP, Sqh-mCherry [25,28] and Mat-Gal4-67,15 (St. Johnston / Cambridge).

Ca^{2+} uncaging and imaging

NP-EGTA, AM (2 mM, Invitrogen) was prepared in 1X injection solution (180 mM NaCl, 10 mM HEPES, 5 mM KCl, 1 mM $MgCl_2$ [pH 7.2])[11]. Embryos (2–2.5 hours at 25°C) were collected for injection. Embryos were incubated at 25°C in dark about 10–20 min prior to uncaging. We employed a 355 nm pulsed YAG laser (DPSL-355/14, Rapp OptoElectonic) mounted on the epiport. We illuminated under the ‘Click and Fire’ Mode on the ‘REO-SysCon-Zen’ platform (Rapp OptoElectonic), while a movie was

recorded on a spinning disc microscope (Zeiss, 100x/oil, NA1.4) with an emCCD camera (Photometrics, Evolve 512). The intensity of the UV laser was adjusted so that no morphological changes were induced in 1X injection solution injected embryos. The laser was applied for 1.5 seconds (around 300 pulses) per cell with 2.5% laser power (~0.5 mJ/cell). For the images in Fig. 2 and 3, axial stacks of 3–4 images with 0.5 µm step size were recording. For myosin II dynamics, axial stacks of 3–4 image with 1 µm step size were recording. The recording started about 0.5 min after Ca^{2+} uncaging. For variation of the focal volume for uncaging, the parameter 'spot-radius' was changed on the 'REO-SysCon-Zen' platform (Rapp OptoElectonic).

Image processing and analysis

The fluorescence intensity of GCaMP6-myr (in Fig. 1) was measured manually with ImageJ/Fiji [29]. The integrated density (a.u.) was measured along the cell membrane and normalized by the cell membrane length (µm) to get the normalized fluorescence intensity I_t. The background I_b was from the integrated density (a.u.) which are measured from the cytoplasm and normalized by the measurement length (µm). The normalized GCaMP6 intensity fold increase was calculated as follows:

$$F/F_0 = (I_t - I_b) / (I_{-1} - I_{-1b})$$

Where I_t is the normalized intensity at time t, I_b is the normalized intensity of the background at time t. I_{-1} is the normalized intensity at 1 second before UV illumination, I_{-1b} is the normalized intensity of the background at 1 second before UV illumination.

Image stacks were projected by the "Max Intensity" option and segmented with "Tissue Analyzer" [30] in ImageJ/Fiji. Cell area measurements were carried out with ImageJ/Fiji. In movie 3, the Z-projected images were stabilized with "Image Stabilizer" [31]. The image stacks from sqh-mCherry embryos were projected with the "Max Intensity" option. Medial myosin II intensity (in Fig. 4) was measured manually with ImageJ.

Acknowledgements

We are grateful to Marion Silies, Stefan Luschnig, Adam Martin, and Daniel St Johnston for materials. We acknowledge service support from the Bloomington Drosophila Stock Center (supported by NIH P40OD018537). This work was in part supported by the Göttingen Centre for Molecular Biology (funds for equipment repair) and the Deutsche Forschungsgemeinschaft (DFG, FOR1756 GR1945/6-1/2, SFB937/TP10 and equipment grant INST1525/16-1 FUGG).

Author contributions

DK conducted the experiments and analyzed the data. FW, JG conceived and supervised the study. DK, FW and JG wrote the manuscript.

Figure legend

Figure 1 Uncaging induces rapid intracellular Ca^{2+} concentration increase in epithelial target cells. (A) Structure of the cage compound, NP-EGTA complexes with Ca^{2+}. UV illumination cleaves the compound and releases free Ca^{2+}. The photo-labile bond is indicated in red. **(B)** Experimental scheme for Ca^{2+} uncaging in *Drosophila* embryos. “NP-EGTA, AM” was injected into the staged embryos. Following a brief incubation, a selected cell was targeted by a UV laser. Light paths for imaging and UV uncaging were controlled independently (target cell indicated in blue). **(C, D)** Images from time lapse recording of embryos (stage 7) expressing a membrane bound Ca^{2+} sensor (GCaMP6-myr) and injected with (C) 2 mM “NP-EGTA, AM” or (D) with buffer (control). Scale bar 10 µm. **(E)** Fluorescence of GCaMP sensor in the target cell normalized to initial value. Mean (bold line, 3 cells in 3 embryos) with standard deviation of the mean (ribbon band). **(F)** Fluorescence of GCaMP sensor in target cell, 3 next neighbors and 3 non-immediate neighbors. Target cell (red), nearest neighbors (green), next-nearest neighbors (orange). Scale bar 10 µm.

Figure 2: Ca^{2+} uncaging induces cell contraction. Images from a time-lapse recording of epithelial cells in embryos (stage 7) expressing E-Cad-GFP, injected with

(A) 2 mM “NP-EGTA, AM” (blue) or **(B)** buffer (purple) and exposed to the UV laser. Scale bar 10 µm. Target cells are highlighted. **(C)** Cross-sectional area of target cells normalized to initial size. Mean (bold line) with standard deviation of the mean (ribbon band). Uncaging, (blue) 8 cells in 8 embryos. Control (purple) 5 cells in 5 embryos. **(D, E)** Cross-sectional area of a target cell (highlighted in blue) with extended recording over 15 minutes after a Ca^{2+} uncaging. Scale bar, 10 µm.

Figure 3: Focal volume of UV exposure affects response time. (A) Target cells were exposed to UV light with a large or small focal volume by adjusting the spot radius. **(B)** Images from a time-lapse recording of epithelial cells in embryos (stage 7) expressing E-Cad-GFP and injected with 2 mM “NP-EGTA, AM”. Two target cells were exposed to the UV laser one after the other with a spot radius of 4 (purple) or 1 (blue). Scale bar 10 µm. **(C)** Traces of cross sectional area of target cells normalized to the initial area in each of three cells in three embryos. Mean (bold) and standard deviation of the mean (ribbon band).

Figure 4: Myosin II dynamics in target cells. Embryos expressing Sqh-mCherry (green) and E-Cadherin-GFP (red) were injected with **(A)** 2 mM “NP-EGTA, AM” injected or **(B)** buffer. Images from a time-lapse recording in cells of the lateral epidermis in embryos (stage 7) after UV exposure at indicated times. Yellow arrowheads point to target cells. Scale bar 10 µm. **(C)** Quantified medial Sqh-mCherry fluorescence intensity in target cells. The change in fluorescence intensities with reference to fluorescence in the first frame after UV-laser illumination is plotted for the target cells. Mean of three cells in 3 embryos (bold line) and standard deviation of the mean (ribbon).

Movie 1: Uncaging induces rapid intracellular Ca^{2+} concentration increase in epithelial target cells. Time-lapse recording from epithelial cells in stage 7 embryos were expressing UAS-myr-GCaMP6, driving by maternal GAL4. Ca^{2+} uncaging was applied in a single cell at t = 0. A stack was acquired every second. Time is indicated as minutes: seconds. Anterior left, dorsal up. This movie relates to Fig. 1C.

Movie 2: Ca^{2+} uncaging induces rapid contraction of epidermal cells. Time-lapse recording from epithelial cells in stage 7 embryos were expressing E-Cad-GFP. Ca^{2+} uncaging was applied in a single cell. The target cell is marked by a red dot. A stack was acquired every 5 seconds. Time is indicated as minutes: seconds. Anterior left, dorsal up. This movie relates to Fig. 2.

Movie 3: The contraction response of target cells is controlled with UV-laser illumination size. Time-lapse recording from epithelial cells in stage 7 embryos were expressing E-Cad-GFP. Ca^{2+} uncaging was applied in two target cells simultaneously with different UV-laser illumination sizes. The bottom cell, which was illuminated with big focal volume, showed apical contraction in 1 min (indicated with purple dot). The top cell, which was illuminated with small focal volume, showed apical contraction in 3 min (indicated with blue dot). A stack was acquired every 5 seconds. Time is indicated as minutes: seconds. Anterior left, dorsal up. This movie relates to Fig. 3.

Figure S1: Area traces of target cells. Traces of cross-sectional cell areas of individual target cells (dashed lines) following UV-laser illumination. **(A)** Embryos injected with 2 mM "NP-EGTA, AM" injected embryos (n=8 cells in 8 embryos). **(B)** Embryos injected with buffer (n=5 cells in 5 embryos). Mean (bold line) with standard deviation of the mean (ribbon).

Figure S2: Variation of UV exposure. Exposure by large (purple lines, spot radius 4) and small (blue lines, spot radius 1) focal volume of the UV laser. Cross-sectional cell area of target cells after Ca^{2+} uncaging normalized to the initial size. Each line represents one individual cell in one embryo.

References

1. Bertet, C., Sulak, L. & Lecuit, T. Myosin-dependent junction remodelling controls planar cell intercalation and axis elongation. *Nature* **429,** 667–671 (2004).
2. Blankenship, J. T., Backovic, S. T., Sanny, J. S. P., Weitz, O. & Zallen, J. A. Multicellular Rosette Formation Links Planar Cell Polarity to Tissue Morphogenesis. *Developmental Cell* **11,** 459–470 (2006).
3. Heisenberg, C.-P. & Bella che, Y. Forces in Tissue Morphogenesis and Patterning. *Cell* **153,** 948–962 (2013).

4. Martin, A. C. & Goldstein, B. Apical constriction: themes and variations on a cellular mechanism driving morphogenesis. *Development* **141,** 1987–1998 (2014).
5. Hoffman, B. D. & Yap, A. S. Towards a Dynamic Understanding of Cadherin-Based Mechanobiology. *Trends in Cell Biology* **25,** 803–814 (2015).
6. Guglielmi, G., Barry, J. D., Huber, W. & De Renzis, S. An Optogenetic Method to Modulate Cell Contractility during Tissue Morphogenesis. *Developmental Cell* **35,** 646–660 (2015).
7. Valon, L., Marín-Llauradó, A., Wyatt, T., Charras, G. & Trepat, X. Optogenetic control of cellular forces and mechanotransduction. *Nature Communications* **8,** 14396 (2017).
8. Oakes, P. W. *et al.* Optogenetic control of RhoA reveals zyxin-mediated elasticity of stress fibres. *Nature Communications* **8,** 15817 (2017).
9. Fehrentz, T., Schönberger, M. & Trauner, D. Optochemical Genetics. *Angewandte Chemie International Edition* **50,** 12156–12182 (2011).
10. Lee, H. C. & Auersperg, N. Calcium in epithelial cell contraction. *The Journal of Cell Biology* **85,** 325–336 (1980).
11. Hunter, G. L., Crawford, J. M., Genkins, J. Z. & Kiehart, D. P. Ion channels contribute to the regulation of cell sheet forces during Drosophila dorsal closure. *Development* **141,** 325–334 (2014).
12. Lee, H. & Nagele, R. G. Toxic and teratologic effects of verapamil on early chick embryos: Evidence for the involvement of calcium in neural tube closure. *Teratology* **33,** 203–211 (1986).
13. Smedley, M. J. & Stanisstreet, M. Calcium and neurulation in mammalian embryos. II. Effects of cytoskeletal inhibitors and calcium antagonists on the neural folds of rat embryos. *Journal of Embryology and Experimental Morphology* **93,** 167–178 (1986).
14. Ferreira, M. C. & Hilfer, S. R. Calcium Regulation of Neural Fold Formation: Visualization of the Actin Cytoskeleton in Living Chick Embryos. *Developmental Biology* **159,** 427–440 (1993).
15. He, L., Wang, X., Tang, H. L. & Montell, D. J. Tissue elongation requires oscillating contractions of a basal actomyosin network. *Nature Cell Biology* **12,** 1133–1142 (2010).
16. Suzuki, M. *et al.* Distinct intracellular Ca(2+) dynamics regulate apical constriction and differentially contribute to neural tube closure. *Development* **144,** 1307–1316 (2017).
17. Schneggenburger, R. & Neher, E. Intracellular calcium dependence of transmitter release rates at a fast central synapse. *Nature* **406,** 889–893 (2000).
18. Ellis-Davies, G. C. & Kaplan, J. H. Nitrophenyl-EGTA, a photolabile chelator that selectively binds Ca2+ with high affinity and releases it rapidly upon photolysis. *Proceedings of the National Academy of Sciences* **91,** 187–191 (1994).
19. Burgalossi, A. *et al.* Analysis of neurotransmitter release mechanisms by photolysis of caged Ca2+ in an autaptic neuron culture system. *Nature Protocols* **7,** 1351–1365 (2012).
20. Delaney, K. R. & Shahrezaei, V. Uncaging Calcium in Neurons. *Cold Spring Harbor Protocols* **12,** 1115-24 (2013).

21. Chen, T.-W. *et al.* Ultrasensitive fluorescent proteins for imaging neuronal activity. *Nature* **499,** 295–300 (2013).
22. Fernandez-Gonzalez, R. & Zallen, J. A. Oscillatory behaviors and hierarchical assembly of contractile structures in intercalating cells. *Physical Biology* **8,** 045005–14 (2011).
23. Yu, J. C. & Fernandez-Gonzalez, R. Local mechanical forces promote polarized junctional assembly and axis elongation in Drosophila. *eLife* **5,** 20246 (2016).
24. Vicente-Manzanares, M., Ma, X., Adelstein, R. S. & Horwitz, A. R. Non-muscle myosin II takes centre stage in cell adhesion and migration. *Nature Reviews Molecular Cell Biolog* **10,** 778–790 (2009).
25. Martin, A. C., Kaschube, M. & Wieschaus, E. F. Pulsed contractions of an actin-myosin network drive apical constriction. *Nature* **457,** 495–499 (2009).
26. Gramates, L. S. *et al.* FlyBase at 25: looking to the future. *Nucleic Acids Research* **45,** D663–D671 (2017).
27. Huang, J., Zhou, W., Dong, W., Watson, A. M. & Hong, Y. Directed, efficient, and versatile modifications of the Drosophila genome by genomic engineering. *Proceedings of the National Academy of Sciences* **106,** 8284–8289 (2009).
28. Oda, H. & Tsukita, S. Real-time imaging of cell-cell adherens junctions reveals that Drosophila mesoderm invagination begins with two phases of apical constriction of cells. *Journal of Cell Science* **114,** 493–501 (2001).
29. Schindelin, J. *et al.* Fiji: an open-source platform for biological-image analysis. *Nature Methods* **9,** 676–682 (2012).
30. Aigouy, B., Umetsu, D. & Eaton, S. Segmentation and Quantitative Analysis of Epithelial Tissues. *Methods in Molecular Biology* **1478,** 227–239 (2016).
31. Li, K. The image stabilizer plugin for ImageJ. *http://www.cs.cmu.edu/~kangli/code/Image_Stabilizer.html,* (2008).

Figure 1

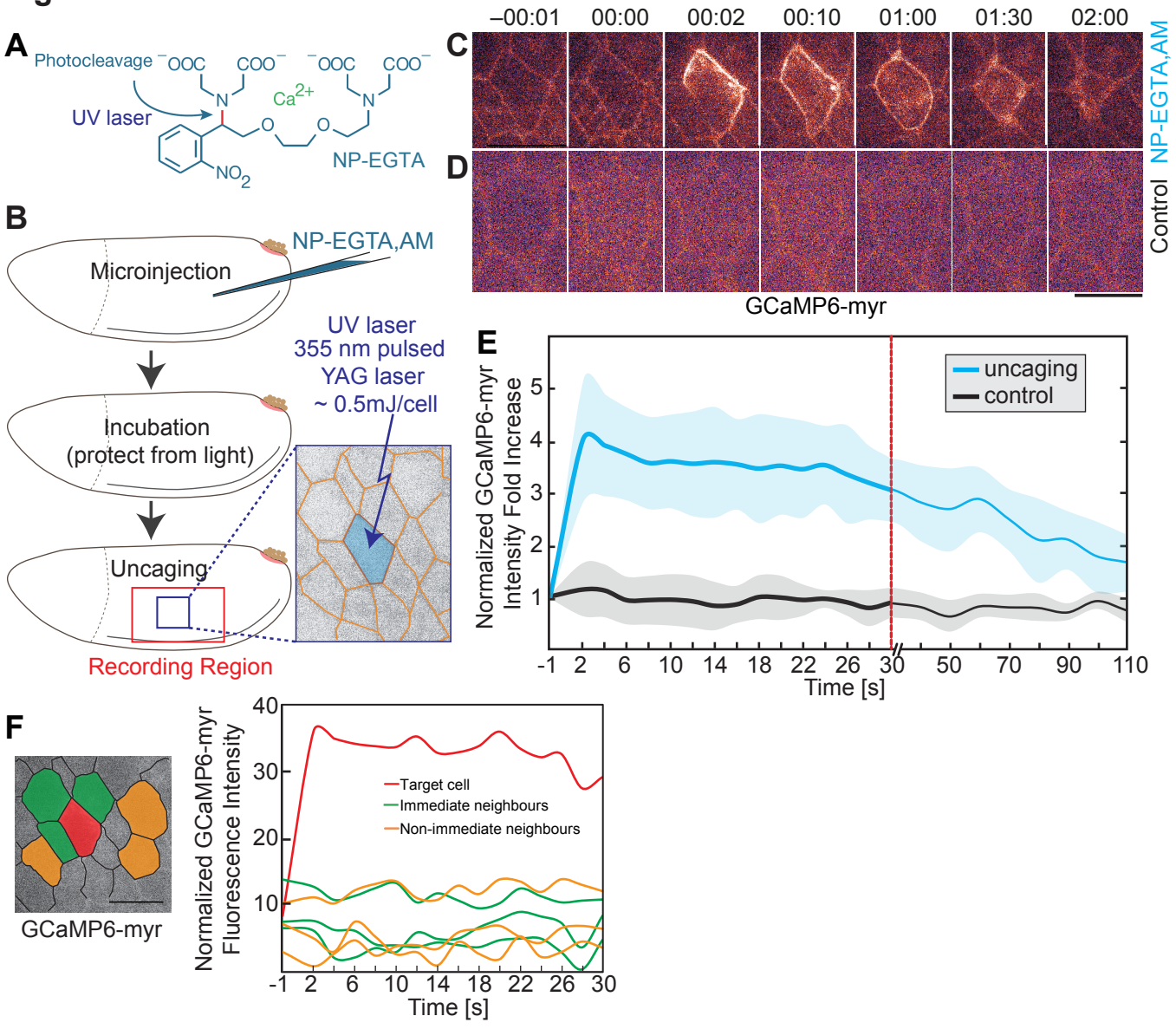
A
Photocleavage
UV laser
Ca2+
NP-EGTA
B
Microinjection
NP-EGTA,AM
Incubation
(protect from light)
Uncaging
UV laser
355 nm pulsed
YAG laser
~ 0.5mJ/cell
Recording Region
C
D
–00:01
00:00
00:02
00:10
01:00
01:30
02:00
NP-EGTA,AM
Control
GCaMP6-myr
E
uncaging
control
Normalized GCaMP6-myr
Intensity Fold Increase
Time [s]
F
GCaMP6-myr
Target cell
Immediate neighbours
Non-immediate neighbours
Normalized GCaMP6-myr
Fluorescence Intensity
Time [s]

Figure 2

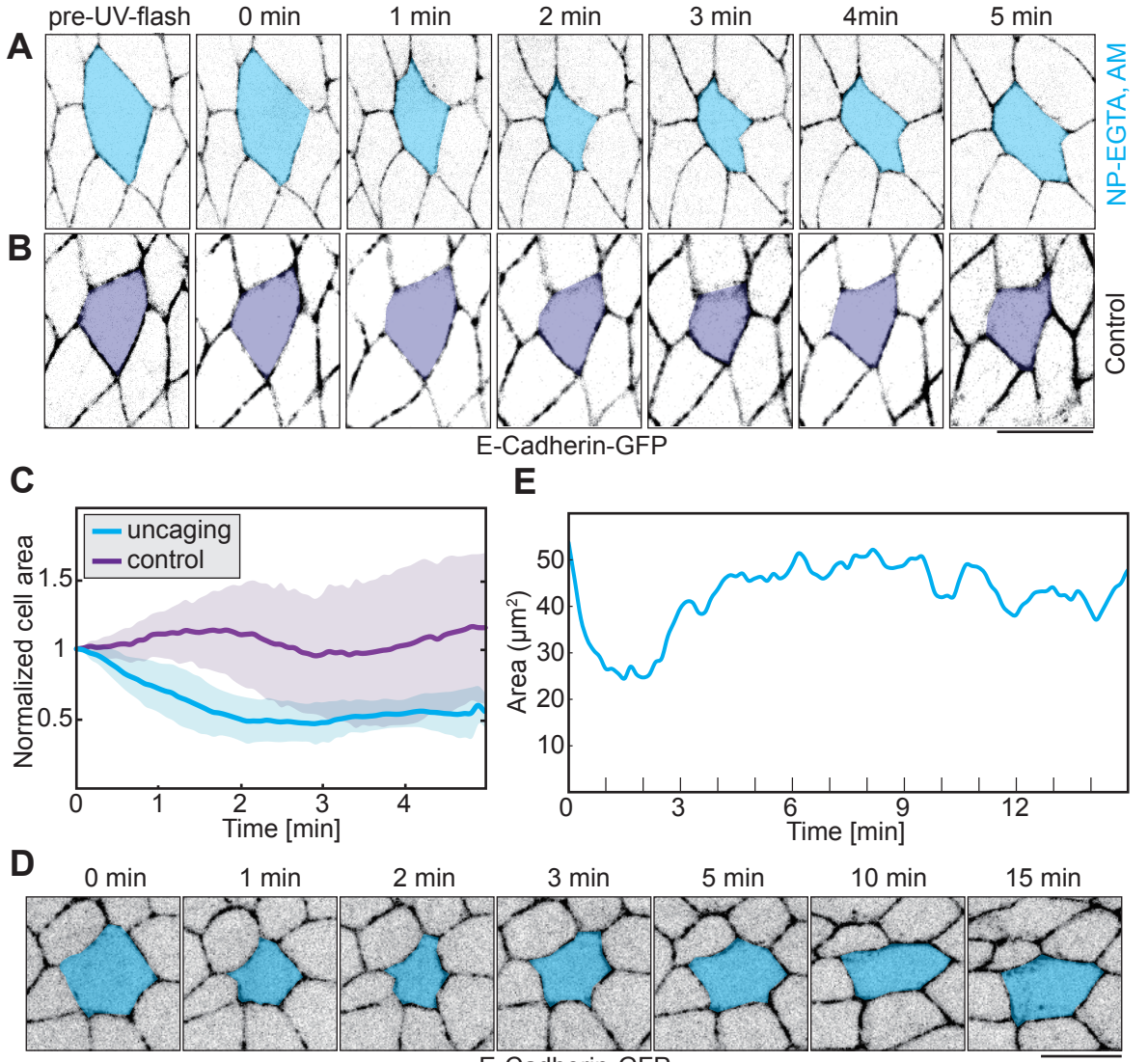
pre-UV-flash
0 min
1 min
2 min
3 min
4min
5 min
A
NP-EGTA, AM
B
Control
E-Cadherin-GFP
C
uncaging
control
Normalized cell area
1.5
1
0.5
0
1
2
3
4
Time [min]
E
Area (μm²)
50
40
30
20
10
0
3
6
9
12
Time [min]
D
0 min
1 min
2 min
3 min
5 min
10 min
15 min
E-Cadherin-GFP

Figure 3

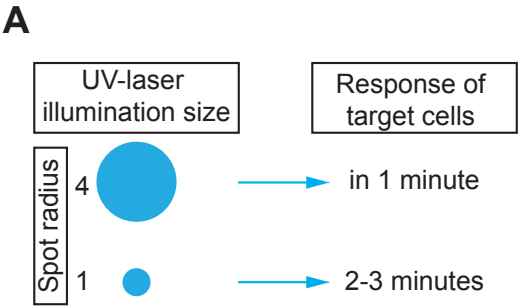
A
UV-laser illumination size
Response of target cells
Spot radius
4
1
in 1 minute
2-3 minutes

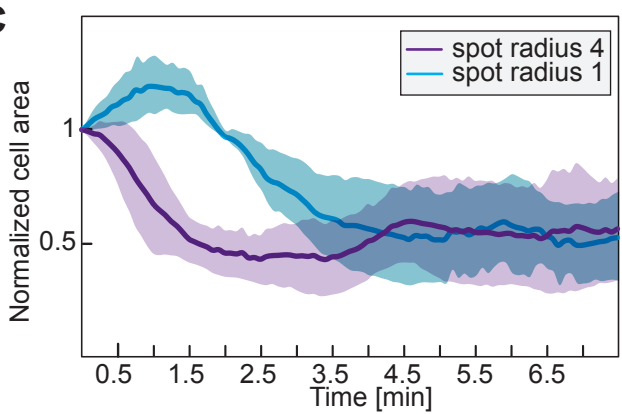
C
spot radius 4
spot radius 1
Normalized cell area
1
0.5
0.5
1.5
2.5
3.5
4.5
5.5
6.5
Time [min]

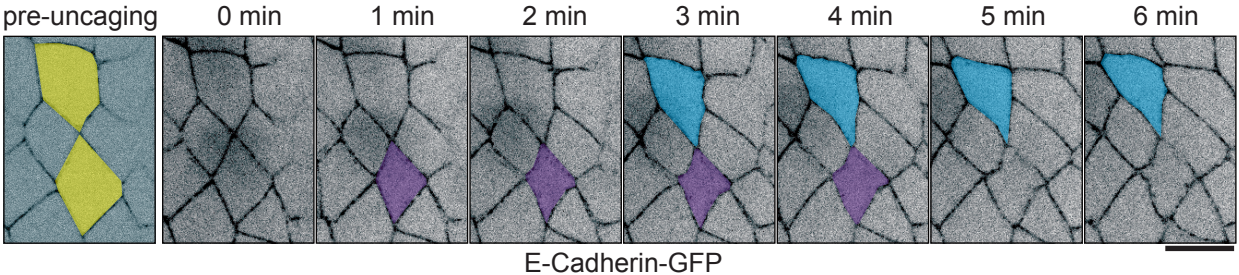
B
pre-uncaging
0 min
1 min
2 min
3 min
4 min
5 min
6 min
E-Cadherin-GFP

Figure 4

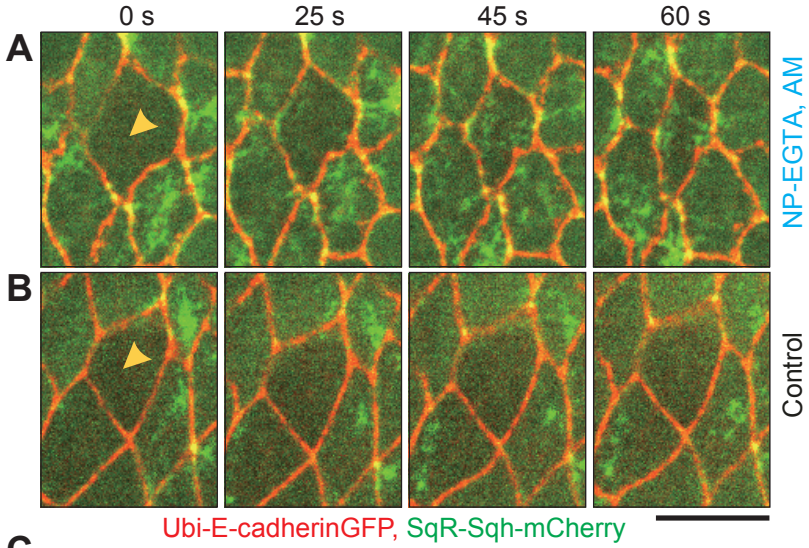
0 s
25 s
45 s
60 s
A
B
NP-EGTA, AM
Control
Ubi-E-cadherinGFP, SqR-Sqh-mCherry

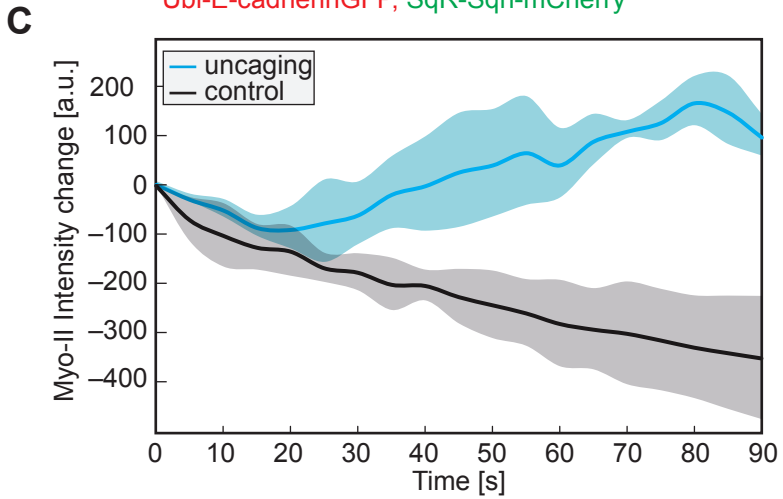
C
uncaging
control
Myo-II Intensity change [a.u.]
200
100
0
−100
−200
−300
−400
0
10
20
30
40
50
60
70
80
90
Time [s]

Figure S1

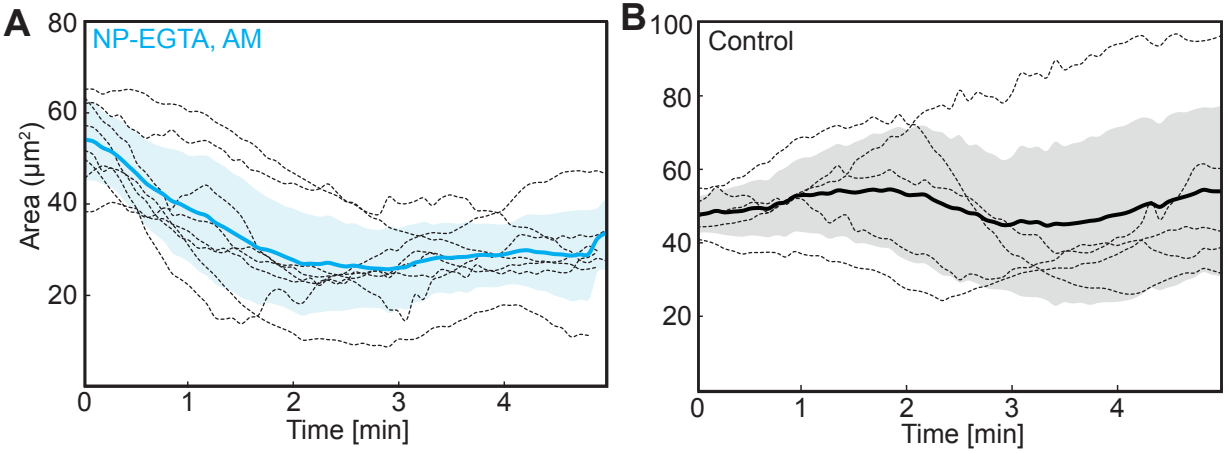
A
NP-EGTA, AM
Area (µm²)
80
60
40
20
0
1
2
3
4
Time [min]
B
Control
100
80
60
40
20
0
1
2
3
4
Time [min]

Figure S2

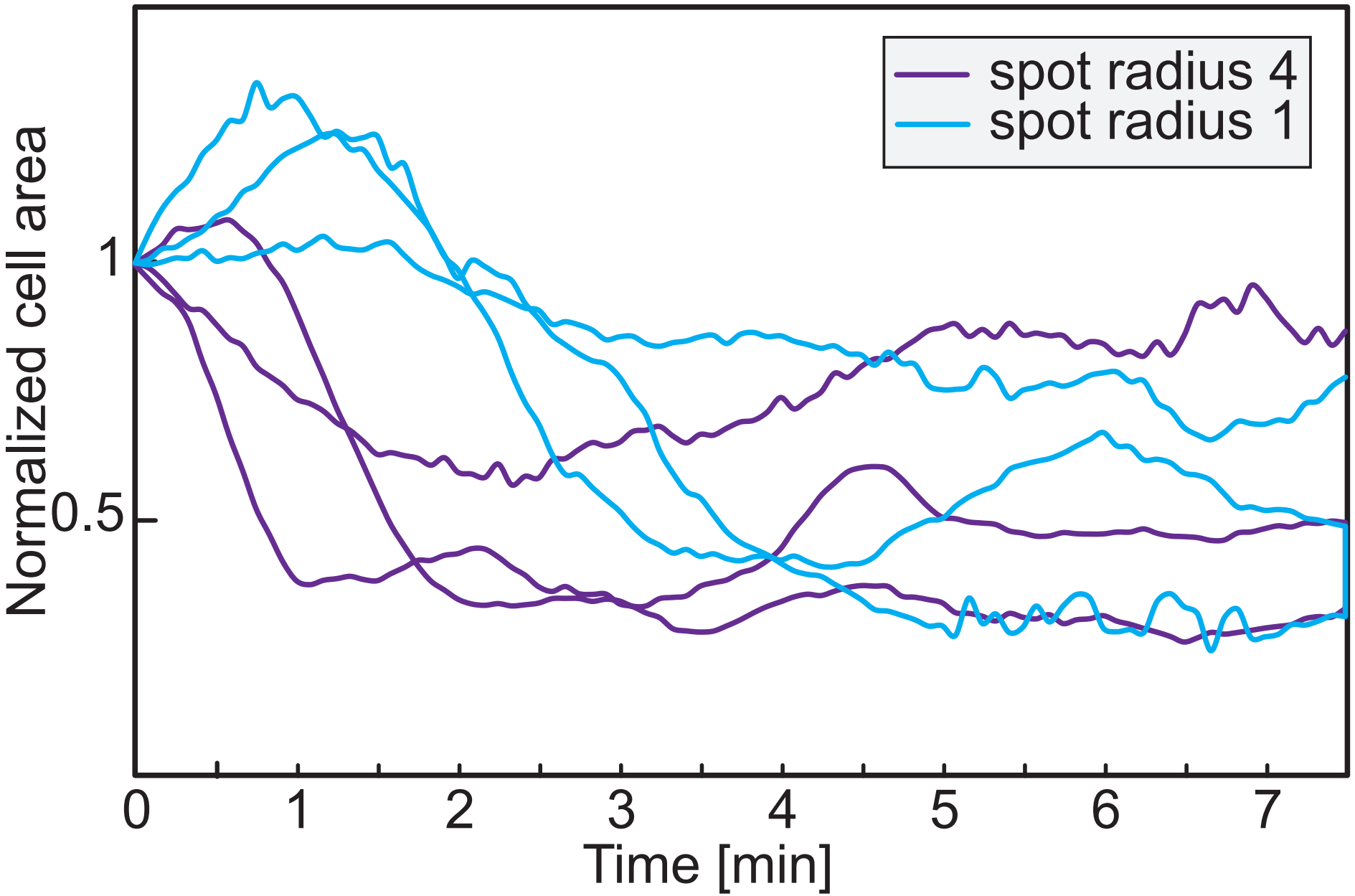
spot radius 4
spot radius 1
Normalized cell area
1
0.5
0
1
2
3
4
5
6
7
Time [min]